Stochastic processes of particle trapping and detrapping by a wave in a magnetized plasma

A. Zaslavsky,[1] C. Krafft,[1] and A. Volokitin[2]
[1]*Laboratoire de Physique des Gaz et des Plasmas, Université Paris Sud, 91405 Orsay Cedex, France*
[2]*Institute of Terrestrial Magnetism, Ionosphere and Radiowave Propagation, Academy of Sciences, Troitsk, Moscow Region 142190, Russia*
(Received 25 July 2005; published 30 January 2006)

This paper presents some relevant numerical simulations of the three-dimensional evolution of a monochromatic lower hybrid wave interacting at the Landau resonance with a Maxwellian electron beam in a magnetized plasma. A statistical study of the stochastic trapping-detrapping transitions performed by a large set of quasiresonant test particles moving self-consistently in the wave's potential has been carried out using dynamical criteria based on simple physical arguments. The paper allows us to explain the role of the stochastic processes at work in the wave-particle interactions and to shed light on their influence on the dynamical evolution of the system over a long range of time.

DOI: 10.1103/PhysRevE.73.016406 PACS number(s): 52.35.Mw

I. INTRODUCTION

A three-dimensional wave-particle Hamiltonian model and the related numerical code have been built recently in order to describe the nonlinear dynamics of electrons in interaction with electrostatic waves in a magnetized collisionless plasma. Some important features characterizing the excitation of such waves at the Landau and the cyclotron resonances by different types of instabilities (fan, loss-cone, bump-in-tail) as well as the accompanying wave-particle and wave-wave nonlinear processes have already been published elsewhere by the authors [1–4]. As the thermal bulk electrons are nonresonant and do not participate directly to the wave-particle interactions, even if they influence the waves through the dielectric tensor, only the resonant particles have been involved in the numerical calculations. Those are performed by a discrete (particle-in-cell) periodic code using symplectic methods to calculate the three-dimensional particles' dynamics self-consistently with the time evolution of the three-dimensional waves' fields.

Considering the case of a single electrostatic wave, it has been observed [1–5] that the total number N of resonant particles used in the discrete numerical calculations influences the long time evolution of the wave amplitude. Typically, when N is increased, the saturation level reached by the wave amplitude due to particle trapping decreases and the slow growth of the wave energy as a function of time during the saturation stage is reduced, which is particularly clear in the long time range. Thus it is important to understand how the discrete character of the particles' distribution can influence the long time evolution of the wave-particle interactions and to determine if the observed N-dependence results from a numerical inaccuracy or from real physical processes. This problem was recently investigated for a one-dimensional single plasma-wave system by comparing, for long time wave-particle interactions, the results provided by a Vlasov-Poisson kinetic approach and a Hamiltonian finite-N one-dimensional system [5]; the authors argued that the kinetic approach hides truly physical plasma effects and that the N-dependent long time behavior observed in the numerical simulations should result from the dynamics of the individual particles. However, many questions remain not answered yet, even for the one-dimensional case.

As a discrete N-particles description of the system allows us to follow the full dynamics of the particles in their complex individual interaction with a wave, we argued in a previous paper [1] that some stochastic processes connected with the trapping and the detrapping of particles by the wave should be the main cause of the observed N-dependence of the wave amplitude. In this paper we show with more details and with the help of a statistical study of the resonant wave-particle interactions that the N dependence is not only due to Schottky noise (which is based on the statistical fluctuations of the finite number N of charge carriers) but is also connected with the complex dynamics of the particles moving across the separatrices in the so-called stochastic layer: such particles can escape from the wave potential trough where they are trapped or, inversely, if they are passing (untrapped), they can be caught by the trough.

This paper presents some relevant numerical simulations of the nonlinear evolution of a lower hybrid wave interacting at the Landau resonance with a Maxwellian electron beam in a magnetized plasma. The specificity of our approach consists to carry out a statistical study of the stochastic transitions (or separatrix crossing) performed by a large set of quasiresonant test particles moving self-consistently in the potential trough of the wave. Up to now studies were mainly conducted considering one or several test particles moving in the superposition of a single or a few potentials of fixed or slowly varying amplitudes in magnetized or unmagnetized plasmas [5–13]. Moreover, when investigating self-consistent wave-particle Hamiltonian systems (e.g., Refs. [12–14]), the main interest of the authors was not focused to study the physical consequences of the separatrix crossing processes on the wave's behavior. Thus the present paper is devoted, by using dynamical criteria based on simple physical arguments, to point out and to explain the role of the stochastic processes at work in the wave-particle interactions and to shed light on their influence on the dynamical evolution of the system over a long range of time. Note that this paper is not aimed to support or to develop more general mathematical problems touching this field of investigation.

II. HAMILTONIAN MODEL

A. Theoretical description

The motion of an electron p of mass m_e and charge $-e<0$ in the electric field $\mathbf{E}=-\nabla\varphi=-\nabla\,\mathrm{Re}(\Phi_{\mathbf{k}}e^{i\mathbf{k}\cdot\mathbf{r}-i\omega_{\mathbf{k}}t})$ of a single electrostatic wave is described by

$$\frac{d\mathbf{v}_p}{dt}+\frac{e}{m_e c}\mathbf{v}_p\times\mathbf{B}_0=-\frac{e}{m_e}\mathbf{E}=\frac{e}{m_e}\mathrm{Re}(i\mathbf{k}\Phi_{\mathbf{k}}e^{i\mathbf{k}\cdot\mathbf{r}_p-i\omega_{\mathbf{k}}t}), \tag{1}$$

which can also be presented in the Hamiltonian form as

$$\frac{d\mathbf{P}_p}{dt}=-\frac{\partial H_0}{\partial\mathbf{r}_p},\quad \frac{d\mathbf{r}_p}{dt}=\frac{\partial H_0}{\partial\mathbf{P}_p}=\mathbf{v}_p, \tag{2}$$

where $\mathbf{P}_p=m_e\mathbf{v}_p-e\mathbf{A}_0(\mathbf{r}_p)/c$ is the generalized particle momentum, $\mathbf{r}_p(x_p,y_p,z_p)$ and $\mathbf{v}_p$ are the particle's position and velocity, c is the speed of light; $\Phi_{\mathbf{k}}$ is the Fourier component of the potential $\Phi(\mathbf{r},t)$ corresponding to the wave of frequency $\omega_{\mathbf{k}}$ and wave vector $\mathbf{k}(k_x,k_y,k_z)$. The vector potential can be expressed through the constant ambient magnetic field $\mathbf{B}_0=B_0\mathbf{z}$ as $\mathbf{A}_0(\mathbf{r}_p)=(\mathbf{B}_0\times\mathbf{r}_p)/2$. The Hamiltonian describing the dynamics of a set of N particles is

$$H_0=\sum_{p=1}^{N}\left(\frac{[\mathbf{P}_p+e\mathbf{A}_0(\mathbf{r}_p)/c]^2}{2m_e}-e\,\mathrm{Re}(\Phi_{\mathbf{k}}e^{i\mathbf{k}\cdot\mathbf{r}_p-i\omega_{\mathbf{k}}t})\right). \tag{3}$$

The full self-consistent interaction between the wave and the particles is described using the total Hamiltonian H,

$$H=H_0+\omega_{\mathbf{k}}|C_{\mathbf{k}}|^2, \tag{4}$$

where the normal amplitude $C_{\mathbf{k}}(t)=\alpha\Phi_{\mathbf{k}}(t)\exp(-i\omega_{\mathbf{k}}t)$ provides the expression of the wave energy density $W_{\mathbf{k}}=\omega_{\mathbf{k}}|C_{\mathbf{k}}|^2/V$; $V=L_xL_yL_z$ is the volume of the system (see the simulation box below). In the case considered hereafter of a lower hybrid wave propagating in a cold background plasma, one has $\alpha=\sqrt{\mathbf{k}^2V(\omega_c^2+\omega_p^2)/8\pi\omega_{\mathbf{k}}\omega_c^2}$, where ω_p and ω_c are the electron plasma and cyclotron frequencies, respectively. Then the wave amplitude evolution is described by [1]

$$\frac{\partial C_{\mathbf{k}}}{\partial t}=-i\frac{\partial H}{\partial C_{\mathbf{k}}^*}=-i\omega_{\mathbf{k}}C_{\mathbf{k}}+\frac{ie}{2\alpha}\sum_{p=1}^{N}e^{-i\mathbf{k}\cdot\mathbf{r}_p}. \tag{5}$$

Considering normalized variables (i.e., $\mathbf{v}\to\mathbf{v}/v_*$, $\mathbf{k}\to\mathbf{k}v_*/\omega_c$, $\Phi_{\mathbf{k}}\to e\Phi_{\mathbf{k}}/m_ev_*^2$, where v_* is the characteristic thermal velocity), the Hamiltonian (4) can be written as

$$H=\sum_{p=1}^{N}\left(\frac{1}{2}[\mathbf{P}_p+\mathbf{A}_0(\mathbf{r}_p)]^2-\mathrm{Re}(\Phi_{\mathbf{k}}e^{i\mathbf{k}\cdot\mathbf{r}_p-i\omega_{\mathbf{k}}t})\right)+\frac{N\mathbf{k}^2|\Phi_{\mathbf{k}}|^2}{2p}, \tag{6}$$

where $p=(n_b/n_0)\omega_p^2/(\omega_c^2+\omega_p^2)$ is a small dimensionless parameter which characterizes the electron flux intensity; n_0 is the background plasma density supporting the waves, and n_b the density of the resonant particles ($n_b=N/V$), with $n_b/n_0\ll1$. Moreover, one can check that the total parallel momentum is conserved,

$$\frac{d}{dt}\left(\sum_{p=1}^{N}P_{pz}+\frac{k_z}{\omega_{\mathbf{k}}}\frac{N\mathbf{k}^2|\Phi_{\mathbf{k}}|^2}{2p}\right)=0, \tag{7}$$

where $P_{pz}=\mathbf{P}_p\cdot\mathbf{z}$. Then, using the generating function $F_1(x,y,z,\theta,X,Z)=-\cot\theta(x-X)^2/2-yX+(z-Z)P$ which produces the canonical transformations $\mathbf{p}=\partial_{\mathbf{r}}F_1$, $J=-\partial_\theta F_1$, $Y=-\partial_X F_1$, and $P=-\partial_Z F_1$, we obtain (omitting the index "p")

$$x=X+\sqrt{2J}\sin\theta,\quad y=Y+\sqrt{2J}\cos\theta,\quad z=Z,$$

$$p_x=-\sqrt{2J}\cos\theta,\quad p_y=\sqrt{2J}\sin\theta-x,\quad p_z=P. \tag{8}$$

Therefore in the frame where $\mathbf{A}_0(\mathbf{r}_p)=x_p\mathbf{y}$, we get

$$H=\sum_{p=1}^{N}\left(\frac{P_p^2}{2}+J_p-\mathrm{Re}(\Phi_{\mathbf{k}}e^{i\mathbf{k}\cdot\mathbf{r}_p-i\omega_{\mathbf{k}}t})\right)+\frac{N\mathbf{k}^2|\Phi_{\mathbf{k}}|^2}{2p}, \tag{9}$$

where J_p and P_p are defined owing to Eq. (8). Writing that $\exp(i\mathbf{k}\cdot\mathbf{r}_p-i\omega_{\mathbf{k}}t)=\exp\{i(\mathbf{k}\cdot\mathbf{R}_p+\sqrt{2J_p}[k_x\sin\theta_p+k_y\cos\theta_p]-\omega_{\mathbf{k}}t)\}$, where $\mathbf{R}_p=(X_p,Y_p,Z_p)$, and choosing the axes so that $k_y=0$ ($k_x=k_\perp$), the Hamilton equation $dX_p/dt=\partial_Y H_0=0$ leads to $X_p=X_{0p}=cste$. Then, performing the canonical transformations $Z_p'=Z_p+(k_\perp/k_z)X_{0p}$ and $P_p'=P_p$ derived from the generating function $F_{2p}=[Z_p+(k_\perp/k_z)X_{0p}]P_p'$, we can write that

$$e^{i\mathbf{k}\cdot\mathbf{r}_p-i\omega_{\mathbf{k}}t}=e^{i(k_zZ_p'+\sqrt{2J_p}k_\perp\sin\theta_p-\omega_{\mathbf{k}}t)}, \tag{10}$$

and performing a Bessel expansion (J_n is the Bessel function of order n), we get

$$e^{i\mathbf{k}\cdot\mathbf{r}_p-i\omega_{\mathbf{k}}t}=\sum_{n=-\infty}^{+\infty}J_n(\sqrt{2J_p}k_\perp)e^{i(k_zZ_p'+n\theta_p-\omega_{\mathbf{k}}t)}. \tag{11}$$

Extracting in Eq. (11) the Landau resonance term $n=0$, which is justified if there is no particle with a parallel velocity v_z close to a cyclotron resonant velocity $v_R=(\omega_{\mathbf{k}}+n\omega_c)/k_z$ ($n\neq0$), one can express the right hand side of Eq. (11) as $J_0(\sqrt{2J_p}k_\perp)e^{ik_zZ_p'-i\omega_{\mathbf{k}}t}$. If for each particle p one has $\sqrt{2J_p}k_\perp=k_\perp v_{p\perp}/\omega_c\ll1$ ($v_{p\perp}$ is the particle's perpendicular velocity), so that $J_0(k_\perp v_{p\perp}/\omega_c)\simeq1$, Eq. (11) can be reduced to the one-dimensional form

$$e^{i\mathbf{k}\cdot\mathbf{r}_p-i\omega_{\mathbf{k}}t}\simeq e^{i(k_zZ_p'-\omega_{\mathbf{k}}t)}, \tag{12}$$

which shows that for the Landau resonance and for electrons of small Larmor radius compared to the wavelength $2\pi/k_\perp$, one can avoid the effect of the magnetic field in the estimate of the bounce frequency Ω_b of the trapped particles; then the normalized value of Ω_b can be considered to be equal to $\sqrt{k_z^2|\Phi_{\mathbf{k}}|}$. We have verified such a result by comparing the simulation results provided by the three-dimensional (3D) code including the magnetic field with those provided by the corresponding 1D code.

Finally the effective one-dimensional Hamiltonian H describing the wave-particle interaction at the Landau resonance can be written, avoiding in Eq. (9) the constant term Σ_pJ_p and noting Z_p instead of Z_p', as

$$H=\sum_{p=1}^{N}\left(\frac{P_p^2}{2}-\mathrm{Re}(\Phi_{\mathbf{k}}e^{i(k_zZ_p-\omega_{\mathbf{k}}t)})\right)+\frac{N\mathbf{k}^2|\Phi_{\mathbf{k}}|^2}{2p}. \tag{13}$$

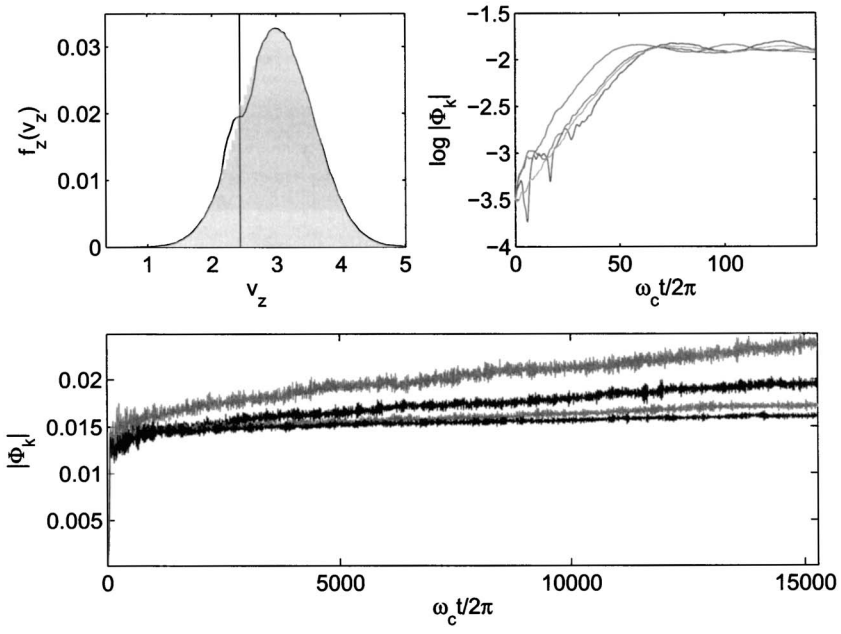

FIG. 1. Upper left panel: superposition of the particles' parallel velocity distribution $f_z(v_z)$ [Eq. (16)] at the initial and the final normalized simulation times, $\omega_c t/2\pi=0$ and $\omega_c t/2\pi=15\,000$, represented by a grey pattern and a solid line, respectively; the vertical line indicates the Landau resonant velocity $v_R=\omega_{\mathbf{k}}/k_z=2.4$; $f_z(v_z)$ and $f_\perp(v_\perp)$ are Maxwellian functions with drift and thermal normalized velocities $v_{z0}=3$, $v_{T_z}=0.8$, $v_{T_\perp}=0.7$. Upper right panel: variation as a function of $\omega_c t/2\pi$ of the normalized wave amplitude $|\Phi_{\mathbf{k}}|$ in logarithmic scale, for $\omega_c t/2\pi \lesssim 150$ (linear interaction stage), and for different values of N: $N=10^5$, 2×10^5, 5×10^5, 10^6. Lower panel: variation as a function of $\omega_c t/2\pi$ of the normalized wave amplitude $|\Phi_{\mathbf{k}}|$ in the full range of time, for different values of N: $N=10^5$ (upper grey curve), $N=2\times10^5$ (upper black curve), $N=5\times10^5$ (lower grey curve), $N=10^6$ (lower black curve). The main normalized parameters are the following: $p=0.02$, $k_z=0.3$, $k_\perp=0.25$, $\omega_{\mathbf{k}}=0.72$.

B. Numerical code

Owing to the Hamiltonian structure of the model, the calculations can be performed using a symplectic mover [15,16] with normalized time steps around $\Delta\tau=\omega_c\Delta t\simeq 0.1-0.2$ whereas checking the numerical accuracy with the help of the energy and the momentum conservations (6), (7). The symplectic property guarantees the preservation of the phase space volumes of the system. As one can separate the Hamiltonian (6) as $H=H_1+H_2$, where

$$H_1=\sum_{p=1}^{N}\frac{(\mathbf{P}_p+\mathbf{A_0})^2}{2}, \tag{14}$$

the symplectic operator of order 2 in time step, $L(\Delta\tau)=L_1(\Delta\tau/2)L_2(\Delta\tau)L_1(\Delta\tau/2)+o(\Delta\tau^3)$, can be used for advancing the Hamiltonian H; L_1 and L_2 are canonical transformations applying to H_1 and H_2, respectively. The transformation L_1 acts on the particles' coordinates and velocities as $\mathbf{r}_p'=\mathbf{r}_p+\hat{T}_{\mathbf{r}}\mathbf{v}_p$ and $\mathbf{v}_p'=\hat{T}_{\mathbf{v}}\mathbf{v}_p$ ($\mathbf{r}_p$ and $\mathbf{v}_p$ are the normalized position and velocity of the particle p) with

$$\hat{T}_{\mathbf{r}}=\begin{pmatrix}\sin(\Delta\tau) & 1-\cos(\Delta\tau) & 0\\ 1-\cos(\Delta\tau) & \sin(\Delta\tau) & 0\\ 0 & 0 & \Delta\tau\end{pmatrix},$$
$$\hat{T}_{\mathbf{v}}=\begin{pmatrix}\cos(\Delta\tau) & -\sin(\Delta\tau) & 0\\ \sin(\Delta\tau) & \cos(\Delta\tau) & 0\\ 0 & 0 & 1\end{pmatrix}. \tag{15}$$

The transformation L_2 for the wave normal amplitude and the particles' velocities is performed keeping constant coordinates, $C_{\mathbf{k}}'=\bar{C}_{\mathbf{k}}(1-e^{-i\omega_{\mathbf{k}}\Delta\tau})+C_{\mathbf{k}}e^{-i\omega_{\mathbf{k}}\Delta\tau}$ and $\mathbf{v}_p'=\mathbf{v}_p-\omega_{\mathbf{k}}\mathbf{k}\{\mathrm{Im}(\bar{C}_{\mathbf{k}}e^{i\mathbf{k}\cdot\mathbf{r}_p})\Delta\tau+\mathrm{Re}[(C_{\mathbf{k}}'-C_{\mathbf{k}})e^{i\mathbf{k}\cdot\mathbf{r}_p}]/\omega_{\mathbf{k}}\}$, where the variables $\omega_{\mathbf{k}}$, $\mathbf{k}$, and $C_{\mathbf{k}}$ are normalized and $\bar{C}_{\mathbf{k}}=\sum_p e^{-i\mathbf{k}\cdot\mathbf{r}_p}$.

III. NUMERICAL RESULTS

A. Wave evolution in a discrete particle distribution

The initial distributions of the parallel and the perpendicular velocities v_z and $v_\perp$ of the resonant particles are modeled by Maxwellian functions

$$f(v_z,v_\perp)=f_z(v_z)f_\perp(v_\perp)=\frac{1}{\pi^{3/2}v_{T_z}v_{T_\perp}^2}\exp\left(-\frac{(v_z-v_{z0})^2}{v_{T_z}^2}\right)\exp\left(-\frac{v_\perp^2}{v_{T_\perp}^2}\right), \tag{16}$$

where v_{T_z} and $v_{T_\perp}$ are the parallel and perpendicular thermal velocities, respectively; v_{z0} is the parallel drift velocity. The resonant electrons are distributed uniformly in space within a numerical box of size $[L_x,L_y,L_z]$ with periodic boundary conditions; this box contains a finite number of wavelengths of each wave present in the system. The electrons are distributed in phase space randomly, or using quiet start methods in order to decrease the Schottky noise; in the latter case, the distributions are sampled using the so-called Hemmersley's sequence. For a given wave, the presented calculations have been performed with a total number of resonant electrons N varying between 10^5 and 10^6.

The evolution with time of a single lower hybrid wave interacting with beam particles has been studied. The Landau resonant velocity $v_R=\omega_{\mathbf{k}}/k_z$ of the considered wave lies in the region of positive slope of the initial parallel velocity distribution function $f_z(v_z)$ so that bump-in-tail instability can occur (see the left upper panel of Fig. 1). Whereas the perpendicular velocity distribution function $f_\perp(v_\perp)$ does not exhibit some significative change as a function of the time—which is expected from the considered resonant mechanism—the final stage of the parallel velocity distribution evolution shows the formation of a narrow plateau in the region where particles interact resonantly with the wave, that is, near v_R. The upper left panel of Fig. 1 presents the superposition of $f_z(v_z)$ at the initial and final simulation times, for

$N=10^6$. In the linear stage of the evolution (see the domain $\omega_c t/2\pi \lesssim 100$ in the right upper panel of Fig. 1), the wave potential amplitude $|\Phi_{\mathbf{k}}|$ increases until saturation, with a normalized growth rate $\gamma_{\mathbf{k}}/\omega_c \simeq 0.01$ which fits well with the theoretical estimate,

$$\frac{\gamma_{\mathbf{k}}}{\omega_c} \simeq \frac{\pi}{2}\frac{p\omega_{\mathbf{k}}}{k^2}A_0 \left.\frac{\partial}{\partial v_z}f_z(v_z)\right|_{v_R}, \tag{17}$$

$$A_0 = \int J_0^2(k_\perp v_\perp) f_\perp(v_\perp) d(\pi v_\perp^2) \simeq 1,$$

that provides approximately the same value $\gamma_{\mathbf{k}}/\omega_c \simeq 0.01$ for the considered conditions. The tiny difference that might appear between the theoretical and the numerical estimates of $\gamma_{\mathbf{k}}$ is due to Schottky noise but also to the fact that the width of the resonance is not very small compared to the width of the beam. Moreover, the final stage of the evolution shows that the average wave amplitude is slowly (in comparison with the linear time $\gamma_{\mathbf{k}}^{-1}$ and the bounce oscillation period Ω_b^{-1} of the trapped particles) and quasilinearly growing with the time (see the lower panel of Fig. 1). Note that this interesting feature characterizing the long time evolution of the nonlinear wave-particle interaction is specific of the kinetic regime and does not appear in the hydrodynamic instability limit [1].

Comparing the variation with time of the wave potential amplitude $|\Phi_{\mathbf{k}}|$ for different values of N, one can observe that the linear growth rate is nearly the same for all the cases (see the upper right panel of Fig. 1). However, a significative difference appears between the simulations after the stage of saturation of the instability, when the process of particles' trapping by the wave begins to take place (see the lower panel of Fig. 1): the slope $d|\Phi_{\mathbf{k}}|/dt$ depends on N in the long time range evolution. This feature is not predicted and not observed for Vlasov-Poisson models where $N \to \infty$ (at least in the one-dimensional case [5]). Figure 2 shows that $d|\Phi_{\mathbf{k}}|/dt \propto N^{-0.7}$ whereas the fluctuations of the wave potential amplitude around its average value,

$$f\langle\Phi_{\mathbf{k}}\rangle = \sqrt{\langle|\Phi_{\mathbf{k}}|^2\rangle - \langle|\Phi_{\mathbf{k}}|\rangle^2}, \tag{18}$$

are roughly scaling as $N^{-0.4}$ (note that the Schottky noise scales as $N^{-0.5}$). Moreover, Fig. 3 shows the Fourier spectrum of these fluctuations computed over the time domain of wave saturation, indicating that the wave amplitude oscillations are controlled by a quite large spectrum of frequencies around the bounce frequency Ω_b: thus their origin should be related to the dynamics of the trapped particles moving in the potential well of the wave, as simple Schottky noise would imply a much wider spectrum of frequencies. Moreover, the effective many-wave field revealed by the Fourier transform is responsible for the chaotic dynamics of the particles moving in the vicinity of the separatrices (trapping-detrapping processes): the dependence of $d|\Phi_{\mathbf{k}}|/dt$ on N is not only due to the Schottky noise but results more significantly from such physical processes. These considerations show that a better understanding of the slow growth and the oscillations of the wave amplitude after the saturation stage requires an accurate study of the individual particles' trajectories.

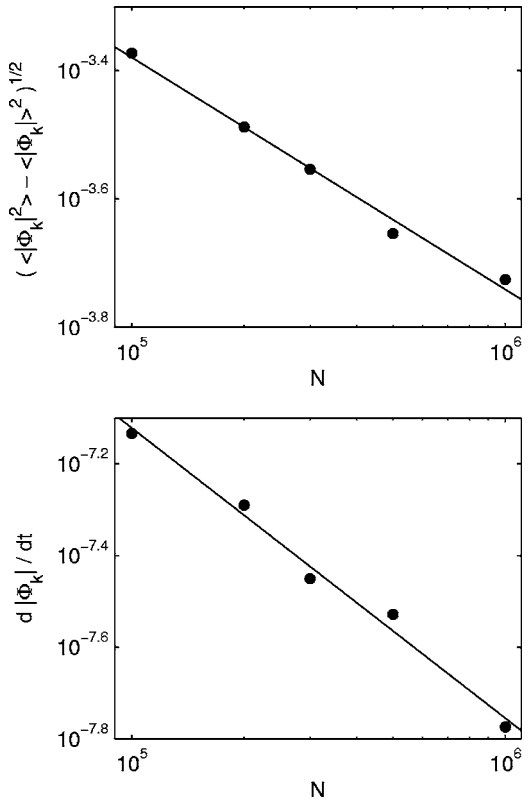

FIG. 2. Upper panel: root-mean-square deviation of the wave amplitude, $f\langle\Phi_{\mathbf{k}}\rangle = \sqrt{\langle|\Phi_{\mathbf{k}}|^2\rangle - \langle|\Phi_{\mathbf{k}}|\rangle^2}$, as a function of N; lower panel: slope $d|\Phi_{\mathbf{k}}|/dt$ of the function $|\Phi_{\mathbf{k}}(t)|$ as a function of N. The full circles correspond to the simulation results and the lines are linear fits. The physical parameters are the same as in Fig. 1.

On the other hand, the wave amplitude correlation function,

$$R(\Delta t) = \langle \mathrm{Re}[\Phi_{\mathbf{k}}(\Delta t)]\mathrm{Re}[\Phi_{\mathbf{k}}(t+\Delta t)]\rangle / \langle \mathrm{Re}[\Phi_{\mathbf{k}}(t)]^2\rangle, \tag{19}$$

has been calculated as a function of the time for different N. Figure 4 shows that, whatever N is, the wave correlations decrease slowly with the time according to a smooth and nonchaotic behavior: the processes of trapping-detrapping take place in a nonstochastically varying wave field so that the only stochasticity to be considered should be connected with the particles' dynamics. Note that the correlations are more strong and stable for large values of N, as the Schottky noise due to the finite number of particles scales as $N^{-1/2}$.

B. Trapping conditions

Let us investigate if the exchange of energy between the wave and the particles performing transitions from being trapped to being untrapped or inversely can influence the wave amplitude evolution over a long range of time. In a first approximation, let us neglect the influence on the wave amplitude of the particles which remain always trapped or always passing, as their trajectories are quasiperiodic,

$$\langle v_{tr}\rangle \simeq 0, \quad \langle v_{ps}\rangle \simeq \mathrm{const}, \tag{20}$$

where the averaging $\langle\ \rangle$ is performed over several bounce periods; v_{tr} (respectively, v_{ps}) is the velocity of a trapped

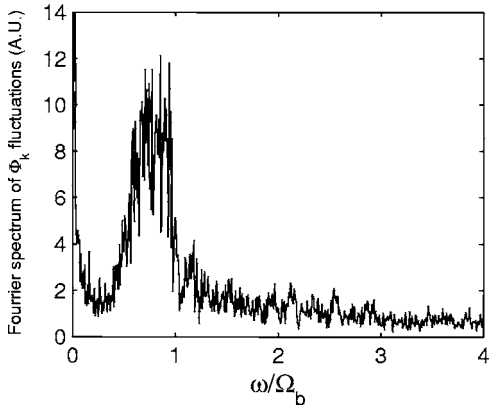

FIG. 3. Fourier spectrum of the wave amplitude fluctuations (in arbitrary units); the frequency ω is normalized to the calculated bounce frequency Ω_b. The Fourier transform has been performed over the time interval $160 \lesssim \omega_c t/2\pi \lesssim 4780$; the quadratic fit of $|\Phi_{\mathbf{k}}(t)|$ has been substracted from $|\Phi_{\mathbf{k}}(t)|$ in order to eliminate the low-frequency components associated with the slow growth of the wave amplitude. The physical parameters are the same as in Fig. 1, with $N=10^5$.

(respectively, untrapped) particle in the frame moving with the wave phase velocity v_φ. Then, considering only electrons close to the separatrices, we can write that [see also Fig. 5(a)]

$$\langle v_{tr} \rangle \simeq 0, \quad \langle v_{ps} \rangle = \pm \frac{\Delta v_R}{2} = \pm \frac{\Omega_b}{k_z}, \tag{21}$$

where Δv_R is the velocity half width between the separatrix maximum and minimum. Then a particle crossing the separatrix, that is, performing a transition, exchanges in average with the wave an amount of kinetic energy $\Delta E_{\mathbf{k}}$,

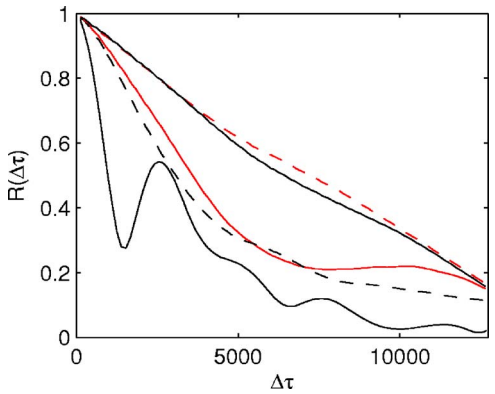

FIG. 4. (Color online) Wave amplitude correlation function $R(\Delta\tau)=\langle \mathrm{Re}[\Phi_{\mathbf{k}}(\tau)]\mathrm{Re}[\Phi_{\mathbf{k}}(\tau+\Delta\tau)]\rangle / \langle \mathrm{Re}[\Phi_{\mathbf{k}}(\tau)]^2\rangle$ calculated as a function of the time $\tau=\omega_c t/2\pi$ for different numbers of particles $N=10^5$ (lower solid curve), 2×10^5 (lower dashed curve), 3×10^5 (middle solid curve), 5×10^5 (upper solid curve), 10^6 (upper dashed curve). The physical parameters are the same as in Fig. 1.

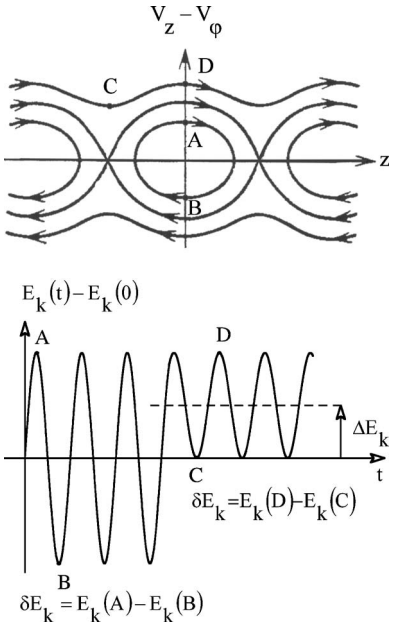

FIG. 5. (a) Schematics of the trajectories of two test particles moving near the separatrices in the $(z, v_z - v_\varphi)$ phase space: the trapped particle moves along a closed line crossing A and B (inside the cat eye) whereas the untrapped particle moves outside the cat eye, crossing the points C and D; (b) variations of the kinetic energy of a test particle, $E_{\mathbf{k}}(t)-E_{\mathbf{k}}(0)$, as a function of the time t; $\Delta E_{\mathbf{k}}$ is the energy jump corresponding to the trapped-detrapped transition; the points A, B, C, and D of (a) are also reported in (b).

$$\Delta E_{\mathbf{k}} = \frac{1}{2}(\langle v_{ps} \rangle + v_\varphi)^2 - \frac{1}{2}(\langle v_{tr} \rangle + v_\varphi)^2$$
$$= \frac{1}{2}\left(\frac{\Omega_b}{k_z}\right)^2 \pm \frac{\Omega_b}{k_z} v_\varphi \simeq \pm \frac{\Omega_b}{k_z} v_\varphi, \tag{22}$$

as $\Omega_b \ll \omega_{\mathbf{k}}$. An electron close to the separatrix can be considered untrapped if its kinetic energy $E_{\mathbf{k}}(t)$ oscillates with an amplitude smaller than half of the width of the cat eye of the potential, i.e., if $\delta E_{\mathbf{k}} \lesssim 2(\Omega_b/k_z)v_\varphi$, where $\delta E_{\mathbf{k}}$ is the absolute value of the difference between two successive extrema of $E_{\mathbf{k}}(t)$ [see Fig. 5(b)], whereas the trapped particles close to the separatrices are verifying the condition $\delta E_{\mathbf{k}} \sim 4(\Omega_b/k_z)v_\varphi$. Note that for deeply trapped particles (far from the separatrices), one has $\delta E_{\mathbf{k}} \lesssim 2(\Omega_b/k_z)v_\varphi$.

The slow growth of the wave amplitude during the saturation stage can be explained by the occurrence of stochastic transitions of particles moving near the separatrices that are successively trapped or detrapped, depending on their dynamics in the oscillating stochastic layer. If more particles are being decelerated than accelerated during the stochastic transitions, then more particles are on average giving energy to the wave than receiving energy from it. As in the initial state the velocity distribution function $f_z(v_z)$ presents a positive slope in the region of the wave phase velocity $v_\varphi = \omega_{\mathbf{k}}/k_z$, one can expect that more particles with higher velocities than the wave $(v_z > v_\varphi)$ will be trapped than particles with smaller velocities $(v_z < v_\varphi)$. To check the validity of this assumption, let us perform a statistical study of

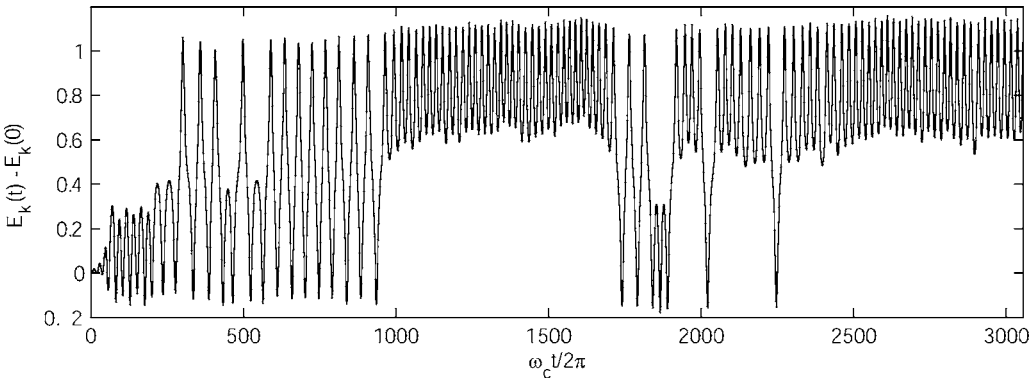

FIG. 6. Variation of the kinetic energy of a test particle, $E_{\mathbf{k}}(t)-E_{\mathbf{k}}(0)$, as a function of the normalized time $\omega_c t/2\pi$. One can see that near $\omega_c t/2\pi \simeq 950$ the particle with $v_z > v_\varphi$ is performing a transition from the state where it is trapped to the state where it is untrapped (the particle is accelerated); near $\omega_c t/2\pi \simeq 1720$, the particle with $v_z > v_\varphi$ is trapped and then detrapped near $\omega_c t/2\pi \simeq 1850$, with $v_z < v_\varphi$. The physical parameters are the same as in Fig. 1.

the trajectories of particles moving in the vicinity of the separatrices.

C. Statistical study

1. Criteria and method

For each simulation result presented below, the trajectories of 5000 test particles selected randomly among the number of particles whose initial parallel velocity v_z verifies $v_\varphi - \Delta v_\varphi \leqslant v_z \leqslant v_\varphi + \Delta v_\varphi$ ($v_\varphi = 2.4$, $\Delta v_\varphi = 0.3$) have been studied (see also Fig. 1). The wave amplitude at the saturation allows us to estimate the resonance width Δv_R around v_φ according to Eq. (21), i.e., $\Delta v_R \simeq 0.22$, justifying the value chosen for Δv_φ which should include the resonance width, the stochastic layer, and some amount of passing particles.

The automatized detection of the stochastic transitions has been carried out as follows. For each test particle, the value $\delta E_{\mathbf{k}}$ [defined above, see also Fig. 5(b)] is calculated along its trajectory. Then, on the basis of the trapping conditions mentioned in the previous section, one can impose a threshold value $\delta E_{\mathbf{k}}^* = 3(\Omega_b/k_z)v_\varphi$ so that the particle is considered as passing (respectively, trapped) if $\delta E_{\mathbf{k}} < \delta E_{\mathbf{k}}^*$ (respectively, $\delta E_{\mathbf{k}} > \delta E_{\mathbf{k}}^*$). The inversion of the sign of the function $\delta E_{\mathbf{k}} - \delta E_{\mathbf{k}}^*$ corresponds to an "event," that is, to a stochastic transition of the test particle between the trapped and the untrapped states. This method provides for each test particle a set of points $\{T_{ev}\}$ corresponding to the times of occurrence of its transitions. Defining $\{\Delta T\}$ as the set of time intervals between two successive transitions, $\Delta T_i = T_{ev,i+1} - T_{ev,i}$, one can calculate the energy jump associated with a transition as the difference of the averaged values of $E_{\mathbf{k}}(t)$ before and after the transition as

$$\Delta E_{\mathbf{k},i} = \frac{1}{\Delta T_i}\int_{T_{ev,i}}^{T_{ev,i+1}} E_{\mathbf{k}}(t)dt - \frac{1}{\Delta T_{i-1}}\int_{T_{ev,i-1}}^{T_{ev,i}} E_{\mathbf{k}}(t)dt, \tag{23}$$

which provides for each test particle a set $\{\Delta E_{\mathbf{k}}\}$ of energy jumps associated with the trapped-untrapped transitions [see also Fig. 5(b)]. We define N_{ev} as the number of events corresponding to a test particle, that is, to the number of values in the set $\{\Delta E_{\mathbf{k}}\}$. This analysis is repeated for each of the 5000 test particles, and the sets $\{\Delta T\}$ and $\{\Delta E_{\mathbf{k}}\}$ are gathered to provide data for a statistical study of all the events detected for all the test particles. For illustration, Fig. 6 shows the variation of the kinetic energy $E_{\mathbf{k}}(t)-E_{\mathbf{k}}(0)$ of a test particle as a function of the normalized time $\omega_c t/2\pi$, pointing out several transitions from trapped to untrapped states or inversely [see also Fig. 5(b)].

2. Results and discussion

Figure 7(a) shows the number of transitions N_{ev} detected as a function of the corresponding calculated energy jumps $\Delta E_{\mathbf{k}} > 0$ and $\Delta E_{\mathbf{k}} < 0$ (the two curves are superposed), for $N = 10^5$ and 5000 test particles. The small enhancement around $|\Delta E_{\mathbf{k}}| \simeq 0$ results from the detection of fake events due to a limitation of the automatized method used to detect the particles' transitions; indeed, in some cases particles are quite deeply trapped by the wave, with $\Delta E_{\mathbf{k}} \sim 3(\Omega_b/k_z)v_\varphi$, and then a small increase of the kinetic energy oscillations' amplitudes, due to processes like adiabatic heating, for example, can be interpreted as a transition; however, the energy jumps associated with such events are nearly zero. One observes that both distributions (for $\Delta E_{\mathbf{k}} > 0$ and $\Delta E_{\mathbf{k}} < 0$) are quite similar, showing that the transitions where a particle takes some energy from the wave or gives some energy to it have roughly the same probability to occur, whatever the total number of particles N is (not shown here). The two vertical lines indicate the calculated value of $\Delta E_{\mathbf{k}} \simeq \Omega_b v_\varphi/k_z \simeq \sqrt{\langle|\Phi_{\mathbf{k}}|\rangle}\omega_{\mathbf{k}}/k_z$ at the beginning of the saturation stage ($\Omega_b v_\varphi/k_z \simeq 0.3$) and at the end of the simulation ($\Omega_b v_\varphi/k_z \simeq 0.37$). It clearly shows that the width of the distribution results from the variation of $\Omega_b \propto \sqrt{\langle|\Phi_{\mathbf{k}}|\rangle}$ over the full saturation stage. Moreover, Fig. 7(b) shows the variation of N_{ev} as a function of $\Delta E_{\mathbf{k}} > 0$, for different values of N: the total number of detected transitions, N_{ev}, as well as the widths of the corresponding distributions decrease when N increases, which is in agreement with the fact that the slope $d|\Phi_{\mathbf{k}}|/dt$ decreases when N increases (see Fig. 2). These histograms allow us to compute the kinetic energy variation of

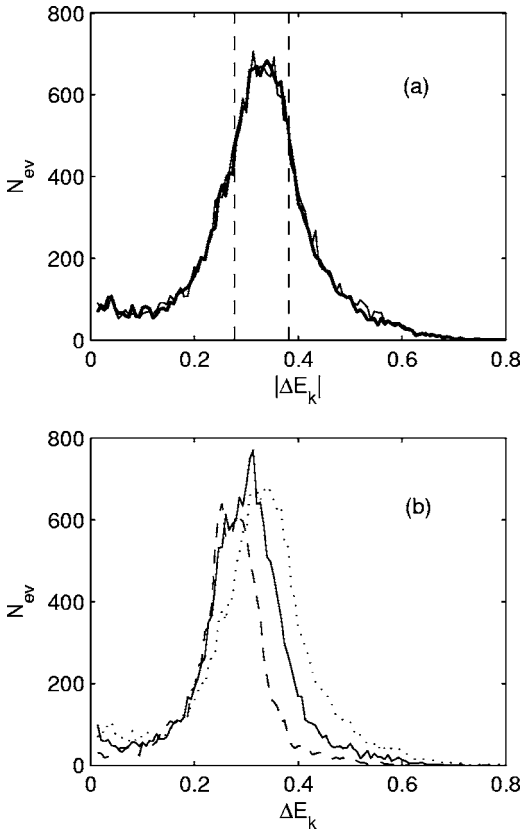

FIG. 7. (a) Superposition of the number of transitions N_{ev} detected as a function of the normalized kinetic energy jump $\Delta E_{\mathbf{k}}$, for $\Delta E_{\mathbf{k}}<0$ (thick solid line) and $\Delta E_{\mathbf{k}}>0$ (thin solid line); the dashed vertical lines represent the values of $\Delta E_{\mathbf{k}}$ calculated using the bounce frequency at the wave saturation time and at the final simulation time; (b) number of transitions N_{ev} detected as a function of $\Delta E_{\mathbf{k}}>0$, for three values of N: $N=10^5$, 2×10^5, and 10^6 (dotted, solid, and dashed lines, respectively). The number of test particles' trajectories examined in each simulation is 5000. The physical parameters are the same as in Fig. 1, with $N=10^5$ for (a).

the sample of 5000 test particles due to stochastic transitions as

$$\Delta\left(\sum_p E_{\mathbf{k}p}\right)_{\text{sample}} \simeq \sum_{\Delta E_{\mathbf{k}}} N_{ev}(\Delta E_{\mathbf{k}})\Delta E_{\mathbf{k}}. \tag{24}$$

Then, assuming that all the particles verifying initially $v_\varphi-\Delta v_\varphi<v_z<v_\varphi+\Delta v_\varphi$ behave like those belonging to the sample, the variation of the particles' resonant energy can be written as

$$\Delta\left(\sum_p E_{\mathbf{k}p}\right) \simeq \frac{N_R}{N_S}\sum_{\Delta E_{\mathbf{k}}} N_{ev}(\Delta E_{\mathbf{k}})\Delta E_{\mathbf{k}}, \tag{25}$$

where N_R is the total number of particles in the resonant domain $[v_\varphi-\Delta v_\varphi, v_\varphi+\Delta v_\varphi]$ and $N_S=5000$ is the number of particles of the sample. The variation of the wave amplitude due to the stochastic transitions of the resonant particles can be evaluated using Eq. (13) while neglecting the potential energy (which is always observed in the simulations to be at least two orders of magnitude below the kinetic and the wave energies)

TABLE I. Comparison between estimations and simulations.

N	$\Sigma_{\Delta E_{\mathbf{k}}} N_{ev}(\Delta E_{\mathbf{k}})\Delta E_{\mathbf{k}}$	$\Delta[\lvert\Phi_{\mathbf{k}}\rvert]_{est}$	$\Delta[\lvert\Phi_{\mathbf{k}}\rvert]_{obs}$	$\sigma(\%)$
10^5	−260	8.5×10^{-3}	9×10^{-3}	5
2×10^5	−141	5.4×10^{-3}	6×10^{-3}	10
5×10^5	−88	3.6×10^{-3}	4×10^{-3}	10
10^6	−89	3.8×10^{-3}	3×10^{-3}	26

$$\Delta\left(\frac{1}{2}\mathbf{k}^2|\Phi_{\mathbf{k}}|^2\right) \simeq -\frac{N_R}{N_S}\frac{p}{N}\sum_{\Delta E_{\mathbf{k}}} N_{ev}(\Delta E_{\mathbf{k}})\Delta E_{\mathbf{k}}, \tag{26}$$

that is

$$\Delta(|\Phi_{\mathbf{k}}|) \sim -\frac{N_R}{N_S}\frac{p}{\mathbf{k}^2\langle|\Phi_{\mathbf{k}}|\rangle N}\sum_{\Delta E_{\mathbf{k}}} N_{ev}(\Delta E_{\mathbf{k}})\Delta E_{\mathbf{k}}, \tag{27}$$

where $\langle|\Phi_{\mathbf{k}}|\rangle$ is the time-averaged value of $|\Phi_{\mathbf{k}}(t)|$. Note that N_R/N is not depending on N and is equal to $\int_{v_\varphi-\Delta v_\varphi}^{v_\varphi+\Delta v_\varphi} f_z(v_z)dv_z \simeq 0.25$ ($\Delta v_\varphi=0.3$), where $f_z(v_z)$ is the normalized electron parallel velocity distribution (16). Table I allows us to compare the normalized values $\Delta[|\Phi_{\mathbf{k}}|]_{est}$ provided by Eq. (27) with the normalized variations $\Delta[|\Phi_{\mathbf{k}}|]_{obs}$ observed in the simulations, for different values of N, where we define the relative error σ as

$$\sigma = \frac{|\Delta(|\Phi_{\mathbf{k}}|)_{est} - \Delta(|\Phi_{\mathbf{k}}|)_{obs}|}{\Delta(|\Phi_{\mathbf{k}}|)_{obs}}. \tag{28}$$

These results show clearly that the observed slow growth of the wave amplitude after the saturation stage is due to the deceleration of particles by the wave trough trapping-detrapping processes. Note that the results are less accurate when N increases (the number of test particles remains constant and equal to 5000 whereas the total number of resonant particles increases from $N_R\sim2.5\times10^4$ to $N_R\sim2.5\times10^5$ when N increases from 10^5 to 10^6).

The time interval ΔT between two successive stochastic transitions does not depend on N and scales as a power law, as shown by Fig. 8,

$$N_{ev}(\Delta T) \propto \Delta T^{-2}. \tag{29}$$

One can estimate the average characteristic time between two successive transitions as

$$\Delta\bar{T} = \frac{\sum_{\Delta T} N_{ev}(\Delta T)\Delta T}{\sum_{\Delta T} N_{ev}(\Delta T)}, \tag{30}$$

which is, for the considered case, of the order of several bounce periods $T_b=\Omega_b^{-1}$: $\Delta\bar{T}\simeq618\tau_c\simeq25T_b=\Delta T_b$ (ΔT is normalized by $\tau_c=2\pi/\omega_c$); note that using the average wave amplitude value $\langle|\Phi_{\mathbf{k}}|\rangle\simeq0.02$ (see Fig. 1) allows us to estimate that $T_b\simeq24\tau_c$. Taking into account the results of Fig. 7 which points out the symmetry of the energy exchanges, Fig. 8 allows us to state that on average no energy exchange between the wave and the particles occurs within a time interval of the order of several ΔT_b.

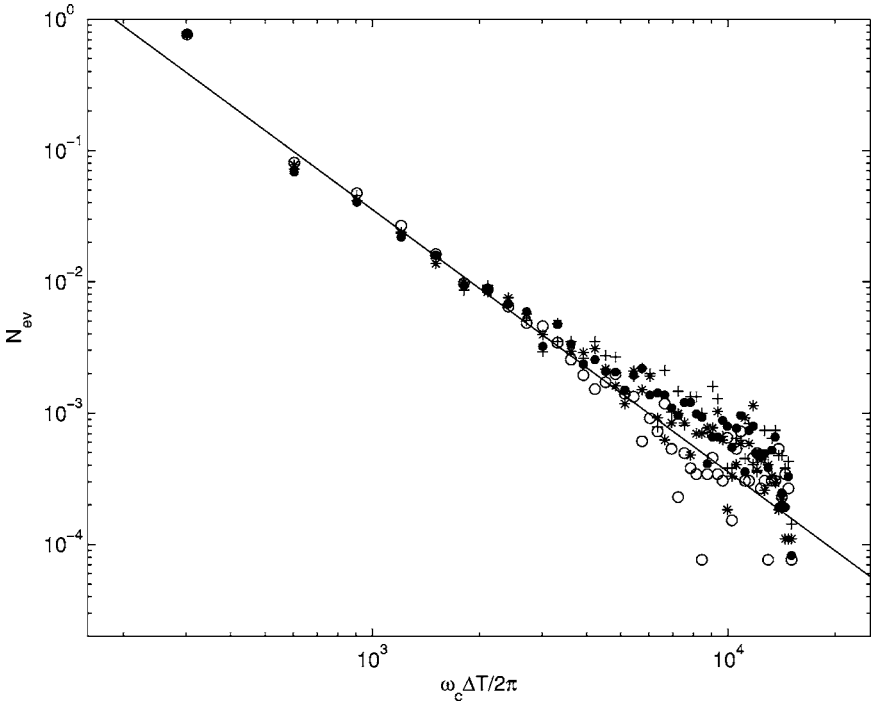

FIG. 8. Variation of the normalized number of transitions N_{ev} as a function of the normalized time interval $\omega_c \Delta T/2\pi$ between two successive transitions, for different values of N: $N=10^5$ (crosses), 2×10^5 (full circles), 5×10^5 (stars), and 10^6 (circles). On this logarithmic plot, the points provided by the simulations are fitted by a linear slope around −2. The number of test particles' trajectories examined in each simulation is 5000. The physical parameters are the same as in Fig. 1.

The variation with time of the number $N_{tr}(t)$ of particles trapped by the wave is presented in Fig. 9. Comparing this figure with the lower panel of Fig. 1 shows that the dependence of N_{tr} on time is exactly correlated to that of the wave potential amplitude $|\Phi_{\mathbf{k}}(t)|$ so that

$$|\Phi_{\mathbf{k}}(t)| \simeq \beta N_{tr}(t), \tag{31}$$

where $\beta \simeq 8\times10^{-6}$, whatever the value of N. This feature can be understood in terms of delayed trapping of particles which are initially far from the stochastic layer: considering that a particle moving in the stochastic layer does not exchange on average any energy with the wave (for time scales of the order of several ΔT_b), which is supported by the results of Fig. 7(a), a net transfer of energy between the wave and the particles is only possible when a particle which is passing at $t<t'$ undergoes its first trapping at $t=t'$, entering by this way in the stochastic layer ($t' \gg \gamma_{\mathbf{k}}^{-1}$) . The Eqs. (22) and (27) allow us to evaluate the wave amplitude variation due to the first trapping of a particle as follows:

$$\Delta[|\Phi_{\mathbf{k}}|]_{1part} \sim \pm \frac{N_R}{N_S} \frac{p v_\varphi}{\mathbf{k}^2 \langle |\Phi_{\mathbf{k}}| \rangle^{1/2} N}. \tag{32}$$

Introducing δ as the probability that the trapping involves an electron of velocity $v_z > v_\varphi$, one can write the average variation of $|\Phi_{\mathbf{k}}|$ due to the trapping at $t=t'$ of a particle passing at $t<t'$ as

$$\Delta[|\Phi_{\mathbf{k}}|]_{1part} \sim \frac{N_R}{N_S} \frac{p v_\varphi}{\mathbf{k}^2 \langle |\Phi_{\mathbf{k}}| \rangle^{1/2} N} (2\delta - 1), \tag{33}$$

which allows us to evaluate the total variation of $|\Phi_{\mathbf{k}}|$ due to the delayed-trapping processes as

$$\Delta[|\Phi_{\mathbf{k}}|] \sim \frac{N_R}{N_S} \frac{p v_\varphi}{\mathbf{k}^2 \langle |\Phi_{\mathbf{k}}| \rangle^{1/2} N} (2\delta - 1) \Delta N_{tr}, \tag{34}$$

where $\Delta N_{tr} > 0$ is the increase of the number of trapped particles inducing the variation $\Delta[|\Phi_{\mathbf{k}}|]$ [Eq. (34)] of the wave amplitude. The function $\Delta N_{tr}(t)$ should be related to the wave's amplitude oscillations around its averaged value and to the slope of the parallel velocity distribution function around the wave phase velocity. Integrating Eq. (34) over the time interval $[t_0, t]$ leads to the estimate (where $t_0 \gg \gamma_{\mathbf{k}}^{-1}$)

$$|\Phi_{\mathbf{k}}(t)| \sim |\Phi_{\mathbf{k}}(t_0)| + \frac{N_R}{N_S} \frac{p v_\varphi}{\mathbf{k}^2 \langle |\Phi_{\mathbf{k}}| \rangle^{1/2} N} (2\delta - 1)[N_{tr}(t) - N_{tr}(t_0)]. \tag{35}$$

In order to be in accordance with the simulation results (31), Eq. (35) should provide that $\delta \simeq 85\%$: the variation of the

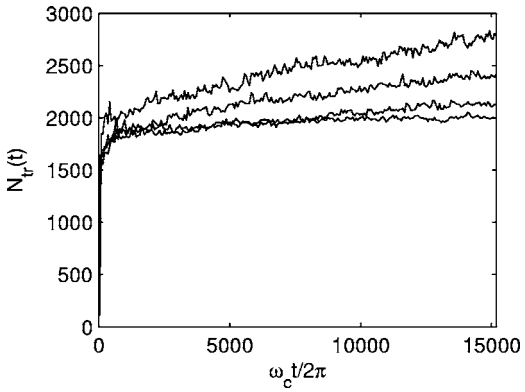

FIG. 9. Variation of the number $N_{tr}(t)$ of particles trapped by the wave as a function of the time $\omega_c t/2\pi$. The values of the total number of particles used in the simulations are $N=10^5$, 2×10^5, 5×10^5, and 10^6 (from the upper to the lower curve, respectively). The number of test particles' trajectories examined in each simulation is 5000. The physical parameters are the same as in Fig. 1.

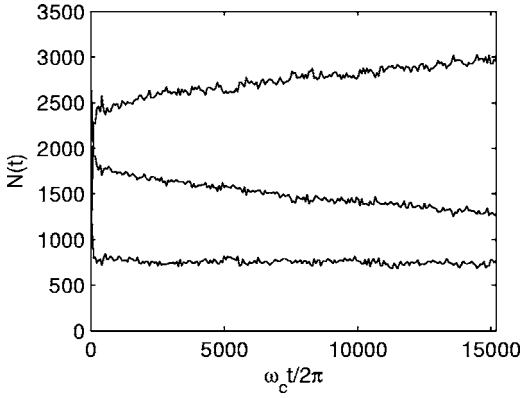

FIG. 10. Variation as a function of $\omega_c t/2\pi$ of the number of trapped particles $N_{tr}(t)$ (upper line), of the number of passing particles $N_{v_z>v_\varphi}(t)$ with a parallel velocity v_z larger than the wave phase velocity v_φ (middle line) and of the number of passing particles $N_{v_z<v_\varphi}(t)$ with $v_z<v_\varphi$ (lower line), for $N=10^5$. The number of test particles' trajectories examined in each simulation is 5000. The physical parameters are the same as in Fig. 1.

wave amplitude can be understood in terms of delayed trapping if 85% of these trapping events are involving passing particles with $v_z>v_\varphi$.

Figure 10 shows that the number of passing particles at the time t whose parallel velocity v_z is smaller than the wave phase velocity v_φ, $N_{v_z<v_\varphi}(t)$, remains roughly constant during all the saturation stage (see the lower curve); meanwhile the passing particles whose velocities v_z are larger than v_φ are "definitively" trapped in the potential well of the wave and their number $N_{v_z>v_\varphi}(t)$ decreases monotonically with the time (see the middle curve) at roughly the same rate as the number $N_{tr}(t)$ of particles trapped by the wave at t grows (see the upper curve). Thus one can evaluate the probability δ as the ratio of the rate of decrease of the passing particles with higher velocities than the wave phase velocity, $\Gamma_{v_z>v_\varphi}=d_t N_{v_z>v_\varphi}$, to the rate of increase of trapped particles, $\Gamma_{tr}=d_t N_{tr}$. In the case of the quasilinear variations observed here, $\Gamma_{v_z>v_\varphi}/\Gamma_{tr}$ can be reduced to the ratio of the variation of the number of passing particles with $v_z>v_\varphi$ to the variation of the number of trapped particles during the same time interval,

$$\delta=-\frac{\Gamma_{v_z>v_\varphi}}{\Gamma_{tr}}=-\frac{\Delta N_{v_z>v_\varphi}}{\Delta N_{tr}}. \tag{36}$$

Using Fig. 10 and Eq. (36) yield that $\delta\simeq 90\%$ for $N=10^5$, which is in good agreement with the estimate of β [Eq. (31)], showing the correlation between the wave amplitude evolution after the saturation and the phenomenon of delayed trapping of particles by the wave. It seems obvious that δ should be related to the slope of the parallel velocity distribution function around the resonant velocity v_R: δ is larger than 50% as there are initially more particles with $v_z>v_\varphi$ than with $v_z<v_\varphi$. For a flat initial distribution, $[\partial f_z(v_z)/\partial v_z]=0$, one should have $\delta=50\%$ and no nonlinear growth of the wave amplitude, as no asymmetry can exist in the trapping of particles. It is possible to evaluate δ on an analytical basis, considering that the probability for a particle to be trapped by the wave is the same for the $v_z>v_\varphi$ and for the $v_z<v_\varphi$ particles: in this case, one should have $\delta\simeq f_z(v_\varphi+\Delta v_\varphi)/[f_z(v_\varphi-\Delta v_\varphi)+f_z(v_\varphi+\Delta v_\varphi)]$, providing $\delta\simeq 75\%$ and $\beta\simeq 6\times 10^{-6}$, which is in good agreement with the observed value $\beta\simeq 8\times 10^{-6}$. Anyway, some additional and not yet explained physical features might be at the origin of the slight difference observed in the probability of trapping of the two groups of particles. Note also that in all the previous evaluations, no possibility of "delayed detrapping" of the particles is considered ($\Delta N_{tr}>0$): as the wave amplitude and thus the width of the potential well increases with the time in the considered physical problem, the probability that an initially trapped (or moving in the stochastic layer) particle becomes "definitively" untrapped can be considered as equal to zero.

Finally, let us discuss the influence of the time step used in the symplectic mover on the rate of occurrence of the stochastic transitions with time. For all the results presented above we used the normalized time step $\omega_c\Delta t=0.2$; moreover, we checked by comparing with simulations performed with $\omega_c\Delta t=0.02$ that the physical results were qualitatively the same and quantitatively quite similar. One just observes that the number of events in Fig. 6 is a little bit underevaluated when using the larger time step, but the shape of the distributions is the same for both time steps. It seems that an extremely weak asymmetry between the $\Delta E_{\mathbf{k}}<0$ and the $\Delta E_{\mathbf{k}}>0$ transitions appears when $\omega_c\Delta t=0.02$ contrary to the case $\omega_c\Delta t=0.2$, but the larger number of events detected for $\omega_c\Delta t=0.02$ can explain this result. For both time steps, the variation of $N_{tr}(t)$ shows a very similar behavior, justifying the use of $\omega_c\Delta t=0.2$ for all the presented simulations.

IV. CONCLUSION

The statistical study based on the simulation results presented above points out some important features of the physical processes governing the self-consistent interactions of a discrete set of N particles with a single wave in a magnetized collisionless plasma. In particular, it demonstrates that the long time evolution of the wave amplitude does not only depend on the Schottky noise effects related to the number of particles in the system, but also on the specific dynamics of the quasiresonant particles moving in the vicinity of the so-called stochastic layer. Indeed, the trapped particles moving in the wave potential well near the separatrices can be detrapped and become passing particles or, inversely, untrapped or detrapped particles in the vicinity of the separatrices can be caught by the wave. Such transitions of particles through the stochastic layer are connected to the fact that the wave amplitude (and thus the potential trough and the related separatrices) is oscillating during the self-consistent interaction of the wave with the deeply trapped particles.

Moreover, the paper shows that the stochastic transitions performed by the quasiresonant particles determine the long time evolution of the amplitude of the wave interacting with the beam electrons. This evolution is shown to be directly

connected to the number of particles trapped by the wave. Applying dynamical criteria to the particles moving near the separatrices, it appears that a test particle moving inside the stochastic layer does not exchange, on a time scale of several bounce periods Ω_b^{-1}, any energy with the wave. Thus the observed net variation of the wave energy during a time scale of the order of thousands Ω_b^{-1} can only be due to the entry in the stochastic layer, after times much larger than the saturation time, of particles initially moving outside the potential well: these particles are considered to undergo a so-called delayed trapping.

Our statistical method allows us to follow the evolution with time of the population of passing particles, showing that the number of delay-trapped particles verifying initially $v_z > v_\varphi$ is larger than the one verifying initially $v_z < v_\varphi$, explaining the increase of the wave energy. This effect is shown to be related to the specific shape of the parallel velocity distribution function destabilizing the wave at the Landau resonance: as $\partial f_z(v_z)/\partial v_z > 0$ around the wave phase velocity, there are more passing particles able to be delay-trapped with $v_z > v_\varphi$ than with $v_z < v_\varphi$. Then, the slope of the wave amplitude growth after the saturation only depends on the function $\Delta N_{tr}(t)$, that is, on the number of delay-trapped events which occurred before the time t. This function has not been studied in detail in the present paper, but should be related to the oscillations of the wave amplitude around its averaged value, $f\langle\Phi_{\mathbf{k}}\rangle = \sqrt{\langle|\Phi_{\mathbf{k}}|^2\rangle - \langle|\Phi_{\mathbf{k}}|\rangle^2}$.

Finally, preliminary studies show that for a three-dimensional cyclotron resonant interaction where the role of the magnetic field is determinant (as the fan instability at the anomalous cyclotron resonance, for example), most of the features described above are relevant. A detailed study of this case will be the subject of a forthcoming paper.

ACKNOWLEDGMENTS

The authors acknowledge the Centre National de la Recherche Scientifique (CNRS, PICS 1310, France), the Institut Universitaire de France (Paris), and the Russian Academy of Sciences for their financial support.

[1] A. Volokitin and C. Krafft, Phys. Plasmas **11**, 3165 (2004).
[2] C. Krafft and A. Volokitin, Ann. Geophys. (Germany) **22**, 2171 (2004).
[3] C. Krafft, A. Volokitin, and A. Zaslavsky, Saturation of the fan instability. Nonlinear merging of resonances (to be published).
[4] C. Krafft, A. Volokitin, and A. Zaslavsky, Saturation of the fan instability. Relaxation of the electron flux (unpublished).
[5] M. C. Firpo, F. Doveil, Y. Elskens, P. Bertrand, M. Poleni, and D. Guyomarc'h, Phys. Rev. E **64**, 026407 (2001).
[6] G. R. Smith, Phys. Fluids **21**, 2253 (1978).
[7] C. R. Menyuk, Phys. Rev. A **31**, 3282 (1985).
[8] A. I. Neishtadt, Sov. J. Plasma Phys. **12**, 568 (1986).
[9] G. R. Smith and A. N. Kaufman, Phys. Fluids **21**, 2230 (1978).
[10] J. R. Cary, D. F. Escande, and J. L. Tennyson, Phys. Rev. A **34**, 4256 (1986).
[11] D. L. Bruhwiler and J. R. Cary, Physica D **40**, 265 (1989).
[12] A. V. Timofeev, Sov. Phys. JETP **48**, 656 (1978).
[13] H. E. Mynick and A. N. Kaufman, Phys. Fluids **21**, 653 (1978).
[14] J. L. Tennyson, J. D. Meiss, and P. J. Morrison, Physica D **71**, 1 (1994).
[15] J. R. Cary and I. Doxas, J. Comput. Phys. **107**, 98 (1993).
[16] J. M. Sanz-Serna and M. P. Calvo, *Numerical Hamiltonian Problems* (Chapman and Hall, London, 1994).